Title

Characterization of Dental Epithelial Stem Cells from the Mouse Incisor with Two-Dimensional and Three-Dimensional Platforms

Journal

Tissue Engineering Part C Methods, 19(1)

ISSN

1937-3384

Authors

Chavez, Miquella G
Yu, Wenli
Biehs, Brian
et al.

Publication Date

2013

DOI

10.1089/ten.tec.2012.0232

Peer reviewed

TISSUE ENGINEERING: Part C
Volume 19, Number 1, 2013

DOI: 10.1089/ten.tec.2012.0232

Characterization of Dental Epithelial Stem Cells from the Mouse Incisor with Two-Dimensional and Three-Dimensional Platforms

Miquella G. Chavez, Ph.D.,[1,2,*] Wenli Yu, D.D.S., Ph.D.,[1,3,*] Brian Biehs, Ph.D.,[1]
Hidemitsu Harada, D.D.S., Ph.D.,[4] Malcolm L. Snead, D.D.S., Ph.D.,[5] Janice S. Lee, D.D.S., M.D., M.S.,[3]
Tejal A. Desai, Ph.D.,[2] and Ophir D. Klein, M.D., Ph.D.[1,6]

Dental epithelial stem cells (DESCs) drive continuous growth in the adult mouse incisors. To date, a robust system for the primary culture of these cells has not been reported, and little is known about the basic molecular architecture of these cells or the minimal extracellular scaffolding that is necessary to maintain the epithelial stem cell population in an undifferentiated state. We report a method of isolating DESCs from the cervical loop of the mouse mandibular incisor. Cells were viable in a two-dimensional culture system and did not demonstrate preferential proliferation when grown on top of various substrates. Characterization of these cells indicated that E-cadherin, integrin alpha-6, and integrin beta-4 mark the DESCs both *in vivo* and *in vitro*. We also grew these cells in a three-dimensional microenvironment and obtained spheres with an epithelial morphology and expression patterns. Insights into the mechanisms of stem cell maintenance *in vitro* will help lay the groundwork for the successful generation of bioengineered teeth from adult DESCs.

Introduction

Engineering of tissues and whole organs holds great promise as a therapeutic tool for the treatment of a variety of developmental disorders as well as tissue damaged by trauma or disease.[1] The tooth is an attractive system for organ regeneration, because it is easily accessible and has a relatively uncomplicated physiology compared with other organs, such as the liver or kidney. In addition, while there is a significant need for replacement teeth in patients with congenital anomalies, victims of trauma, and the elderly, failure of a bioengineered tooth would not be as catastrophic as failure of a larger organ such as a lung or the heart. Thus, teeth provide an important starting point for testing regenerative strategies that could be applicable to other organs.

Two of the principal cell types of the tooth are the dentin-producing odontoblasts, which arise from the neural crest-derived mesenchyme, and the enamel-producing ameloblasts, which arise from the ectodermal epithelium. The field of tooth regeneration has recently made exciting advances, with several groups producing tooth-like structures *in vitro*.[2–4] However, most of this work has focused on understanding the mesenchymal cell populations of the tooth that give rise to odontoblasts[5,6] and on combining mesenchymal stem cells with nondental epithelial populations.[7,8] The rationale for using nondental epithelial cells in these approaches is that humans lose their enamel-producing ameloblasts after tooth eruption,[9] and an ameloblast stem cell population has not been identified in humans.

Although human teeth do not replace enamel after it is initially deposited, a number of mammals, including rodents, have evolved continuously growing teeth.[10] Such teeth provide models for studying the epithelial contribution to enamel regeneration. In rodent incisors, which grow throughout the life of the animal, enamel is formed on the labial (facing the lip) but not lingual (facing the tongue) side,[9] and a sharp tip is formed as a result of preferential abrasion on the lingual surface. Continuous growth of the incisor is driven by pools of adult stem cells. There are two areas within the rodent incisor that are termed the labial and lingual cervical loops, which house epithelial stem cells. A mesenchymal compartment between the two cervical loops is presumed to house the odontoblast stem cells. Little is known about the stem cells in the mesenchymal compartment or the lingual

[1]Program in Craniofacial and Mesenchymal Biology and Department of Orofacial Sciences, [2]Department of Bioengineering and Therapeutic Sciences, and [3]Department of Oral & Maxillofacial Surgery, University of California San Francisco, San Francisco, California.
[4]Division of Developmental Biology and Regenerative Medicine, Department of Anatomy, Iwate Medical University, Morioka, Japan.
[5]Center for Craniofacial Molecular Biology, University of Southern California, Los Angeles, California.
[6]Department of Pediatrics, Institute for Human Genetics, University of California San Francisco, San Francisco, California.
*These two authors are co-first authors.

cervical loop, whereas several studies have demonstrated that the labial cervical loop contains stem cells which differentiate into transit amplifying (T-A) cells and then on to mature enamel-producing ameloblasts as they migrate toward the distal end of the incisor.[11,12] Within the labial cervical loop, there are several different cell types, including inner and outer enamel epithelium, stellate reticulum, and stratum intermedium (Fig. 1A′). The labial cervical loop stem cells reside within the stellate reticulum and the outer enamel epithelium. In addition to ameloblasts, the stem cells are also thought to give rise to other cell types, including the stratum intermedium, which is a single layer just beneath the ameloblasts.

Studying dental epithelial stem cells (DESCs) in the rodent incisor enables a better understanding of both the molecular and physical influences that regulate DESC behavior in the niche as well as how these stem cells differentiate into enamel-producing ameloblasts. In this study, we set out to develop a robust method for harvesting and culturing DESCs using both a two-dimensional (2D) and three-dimensional (3D) platform. For 2D studies, we measured the ability of DESCs to form colonies in the presence or absence of several ECM substrates, as well as the proliferation rates under these conditions. For 3D studies, we measured the efficiency of DESCs to form spheres (amelospheres); the formation of such spheres has been used as an assay for stem cells in neural and mammary systems.[13] Sphere formation allows stem cells to be passaged in an undifferentiated state and to retain their ability to differentiate.[14–16] For both the 2D and 3D studies, we assayed the expression of several cell surface proteins expressed in the cervical loop *in vivo*, and their expression pattern was compared with two dental cell lines, HAT-7 and LS8. The identification of reliable markers for stem cells and an understanding of the processes that enable the manipulation of stem cells *in vitro* are important first steps in dental tissue engineering.

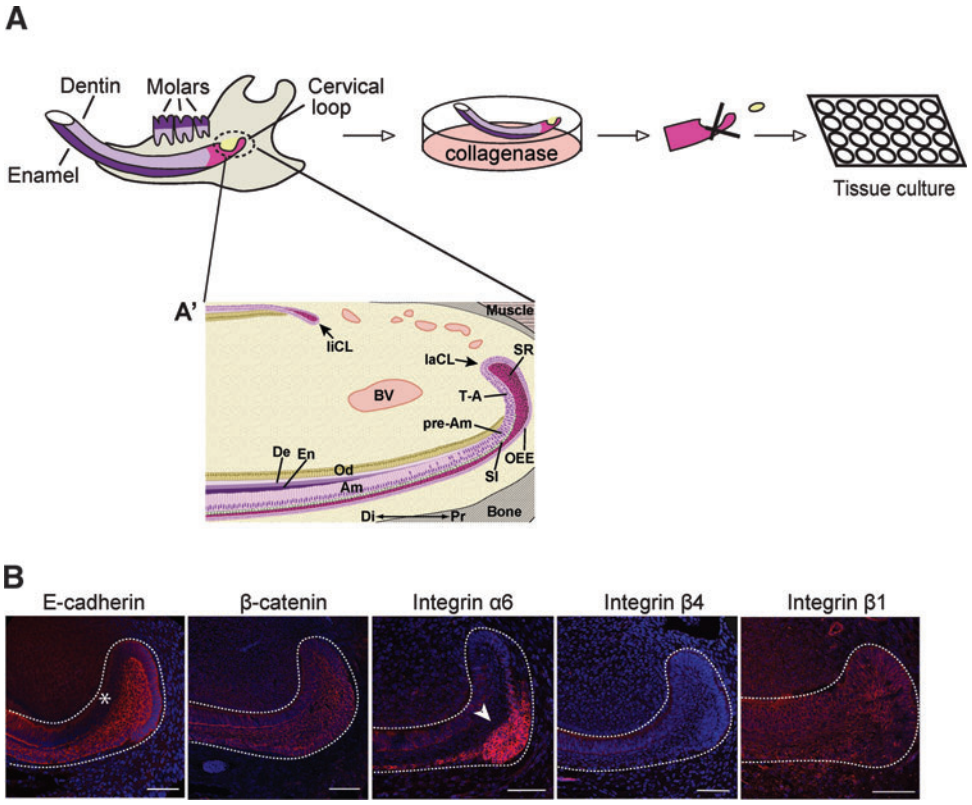

FIG. 1. Workflow of dental epithelial cell primary culture and cell adhesion expression in cervical loop. **(A)** The cervical loop is found at the proximal end of the mandibular incisor. In order to collect stem cells, the jaw was dissected, the bone was removed to expose the incisor with cervical loop intact, and the tooth organ was placed in 2% collagenase to separate the epithelium from the mesenchyme. After 4 h of incubation, the cervical loop was manually excised, dissociated into single cells, and cultured on top of standard tissue culture plates. **(A′)** Schematic of the proximal end of the adult mouse mandibular incisor (sagittal section). Stem cells reside in the stellate reticulum and outer enamel epithelium, and they give rise to T-A cells. T-A cells give rise to preameloblasts, which then further develop into enamel-producing ameloblasts. Am, ameloblasts; BV, blood vessel; De, dentin; Di, distal; En, enamel; laCL, labial cervical loop; liCL, lingual cervical loop; pre-Am, preameloblasts; Od, odontoblasts; OEE, outer enamel epithelium; Pr, proximal; SI, stratum intermedium; SR, stellate reticulum; T-A, transit-amplifying. **(B)** Immunofluorescent staining for adherens junctions and integrins in the cervical loop. Seven micrometer sections were taken from adult mandible incisors and stained for E-cadherin, beta-catenin, and integrins alpha-6, beta-1, and beta-4. Note the general epithelial staining for beta-catenin and integrin beta-1. E-cadherin is absent from the T-A region (asterisk), whereas integrin alpha-6 is restricted to the stellate reticulum and outer enamel epithelium (arrowhead), and integrin beta-4 is restricted to the outer area of the entire cervical loop. Scale bar = 50 μm. Color images available online at www.liebertpub.com/tec

Methods

DESC isolation

Mouse strains CD-1 or C57BL/6N (B6), both from Charles River, were used in this study, and all experiments were approved by the Institutional Animal Care and Use Committee (IACUC) at the University of California, San Francisco (Protocol Number AN084146-02E). The lower incisors were dissected from mouse mandibles and treated with 2% collagenase type I (Worthington Biochemical Company) for 4 h at 4°C. The epithelium was mechanically separated from the mesenchyme, and the apical bud of the epithelium was excised. The excised apical bud tissue was dissociated with Accumax™ (Sigma-Aldrich) at 37°C for 30 min and dispersed by gentle pipetting to generate a single cell suspension.[17] Two cervical loops generally produced around 15,000 cells. Aliquots of the single cell suspension were counted with a hemocytometer. Cells were maintained in culture at 5% CO_2 in medium (DMEM/F12; Invitrogen), supplemented with B27 (Invitrogen), mouse EGF recombinant protein (20 ng/mL; R&D), FGF2 recombinant protein (25 ng/mL; R&D), and 1% antibiotics (penicillin, 100 U/mL, streptomycin, 50 μg/mL).

3D culture of DESCs

To generate the "amelospheres," the cells were plated in ultralow attachment plates with Matrigel (Corning) at a density of 20,000 viable cells/mL in primary culture. Cells were grown in the serum-free medium just described. Amelospheres were collected by gentle centrifugation (800 rpm) after 7–10 days, enzymatically dissociated in 0.25% trypsin for 10 min, and replated at 1000 cells/mL for passaging. For immunostaining experiments, the culture medium with amelospheres was collected into 15 mL polypropylene conical tubes, and the amelospheres were allowed to settle by centrifugation at 400 *g* for 30 min. The supernatant was removed, and 2 mL of 4% phosphate-buffered paraformaldehyde (PFA) was added for 30 min. The amelospheres were rinsed thrice in phosphate-buffered saline (PBS). Immunocytochemistry was performed on intact amelospheres at this stage. For an analysis of the amelosphere sections, the amelospheres were allowed to settle in 50% sucrose at 4°C overnight and embedded in O.C.T. compound (Sakura Tissue-Tek), cut at 5–8 μm thickness, and collected for analysis. Sphere-forming ability across various concentrations was evaluated using one-way analysis of variance (ANOVA).

Colony-forming assay

Colony formation was measured by fixation with 0.5% crystal violet (w/v) in 6% glutaraldehyde. Colonies were then either directly counted, or in cases with colonies overcrowding the well, dye was diluted out with 2% sodium dodecyl sulfate (SDS) solution, and then absorbance was measured at 590 nm as an indirect comparison for colony formation. Statistics comparing colony formation between two mouse strains was evaluated using the Student's *t*-test. Colony formation on various ECM substrates at various concentrations was evaluated using one-way ANOVA with Dunnett's multiple comparison test.

Cell proliferation

Cellular proliferation was assessed using either the CyQuant assay (Invitrogen), which measures DNA content, or the MTT (3-(4,5-dimethylthiazol-2-yl)-2,5-diphenyltetrazolium bromide) assay (Sigma-Aldrich), which measures metabolic activity as an indirect measurement of proliferation. Cyquant assay was performed following the manufacturer's instructions. For the MTT assay, media were removed from the cells and replaced with 100 μL of fresh growth media and 16.5 μL of the MTT reagent (0.8 μg/ul); the plate was incubated for another 4 h; formazan crystals were dissolved in the solubilization solution; and absorbance was measured at a wavelength of 570 nm with a background subtraction at 650 nm. Doubling time was calculated by plotting cell number and using the formula for exponential growth: doubling time = $(\log^2)$/slope.

Western blots

Cells were lysed with SDS lysis buffer (10 mM Tris pH 7.5, 1% SDS, 5 mM EDTA, 2 mM EGTA, 1 mM phenylmethanesulfonylfluoride, 1 μg/mL leupeptin, and 1 μg/mL pepstatin A). Total protein was determined by bicinchoninic acid colorimetric assay (Pierce), and equal amounts of lysate were loaded at 10 μg/lane on a 4%–12% NuPage Bis-Tris gel (Invitrogen). Size-resolved protein was transferred onto nitrocellulose or polyvinylidene fluoride membrane using the iBlot system or wet transfer system following manufacturer's instructions (Invitrogen). Equal loading was ensured by staining membranes with Ponceau S Solution (Sigma). Membranes were blocked in 5% (w/v) milk solution for 1 h at room temperature and then incubated at 4°C overnight with one of the following antibodies: E-cadherin (Invitrogen; clone ECCD-2), beta-catenin (Santa Cruz; clone H-102), integrin alpha-6, (Santa Cruz; clone H-87), integrin beta-1 (Santa Cruz; clone N-20), and integrin beta-4 (Millipore; clone 3E1), all at a 1:1000 dilution. Membranes were washed thrice with Western blot buffer (50 mM Tris, 150 mM NaCl, 0.05% Tween-20); then, secondary antibodies were added at 1:5000 dilutions for 1 h at room temperature. Membranes were washed thrice with Western blot buffer and developed with a Supersignal chemiluminescent detection system (Pierce).

Immunofluorescence

Cells were seeded on 12 mm glass coverslips in a 48-well plate and allowed to grow to subconfluence. The cells were fixed with 4% PFA for 10 min and then Triton permeabilized for an additional 5 min. The cells were blocked with 3% (w/v) bovine serum albumin for 1 h at room temperature. Primary antibodies were added at a 1:100 dilution and included the following: E-cadherin (Invitrogen; clone ECCD-2), beta-catenin (Santa Cruz; clone H-102), integrin alpha-6 (Santa Cruz; clone H-87), integrin beta-1 (Santa Cruz; clone N-20), and integrin beta-4 (Millipore clone 3E1). After an overnight incubation of the primary antibody at 4°C, coverslips were washed thrice in PBS with Tween-20. Secondary antibodies were added and incubated for 1 h at room temperature. The cells were washed thrice with PBS with Tween-20, then mounted onto a glass coverslip with Prolong antifade mounting medium (Invitrogen) either with or without DAPI to stain nuclear DNA. Controls with no primary antibody

were done in parallel, and no staining was visible. Images were taken with either a Leica upright or a confocal microscope TCP SP5.

Quantitative polymerase chain reaction

RNA was isolated with the RNeasy kit (Qiagen) following the manufacturer's instructions. cDNA was synthesized from total RNA with the iScript cDNA synthesis kit (BioRad). Primers were designed using the NCBI Primer BLAST program. Quantitative polymerase chain reaction (qPCR) was performed using GoTaq qPCR Master Mix (Promega) in an Eppendorf Mastercycler Realplex (Eppendorf). qPCR conditions were as follows: 95°C for 2 min, 40 cycles of 95°C 15 s, 60°C 15 s, 68°C 20 s, followed by a temperature gradient. Expression levels of the genes of interest were normalized to the level of the ribosomal RNA L19.

Results

Two well-established criteria for the identification of adult stem cells *in vitro* are colony-forming unit assays and capacity for self-renewal,[18,19] and these were used to evaluate dental epithelial cells. Colonies were observed ~5 days after plating on tissue culture polystyrene (TCPS) (Fig. 2A). In these colonies, the cells had a tightly packed circular morphology that was typical of stem cell colonies. In rare cases, a separate cell type was able to grow that was morphologically different from the typical colonies (data not shown). These rare cells (data not shown) were loosely packed and were morphologically similar to a population reported in studies of epidermal stem cell colonies as being more differentiated cells.[20] Plating efficiency was defined as the ratio of the number of colonies formed to the number of cells seeded.[18] Two different mouse strains were used (B6 and CD-1), and both were able to form colonies (Fig. 2B), with no statistical difference (Student's *t*-test) in plating efficiencies between strains. Cells were seeded at varying concentrations, and proliferation rate was determined (Fig. 2C). Cells plated at a low density (5×10^3/well) proliferated slowly, with a doubling time calculated as 38 days. A 10-fold increase in the number of cells (5×10^4/well) resulted in a shortening of the doubling time to 2.64 days. Self-renewal was assessed by the ability of single cells from dissociated colonies to undergo secondary colony formation. Cells retained the capacity to form colonies at least 10 times during serial passaging (p0–p9), indicating their competence to undergo self-renewal for an extended period of time in culture.

Next, the cells were plated on top of various substrates to determine whether the addition of an extracellular matrix protein could increase colony formation. Surprisingly, no ECM component performed better than TCPS alone in colony formation assays (Fig. 2D), although, as expected, higher colony formation occurred with higher seeding densities. These results were confirmed with an MTT assay, which measures the metabolic activity of cells and is a surrogate for cell proliferation (data not shown). Together, these data indicate that matrix composition in 2D does not have major effects on DESC proliferation.

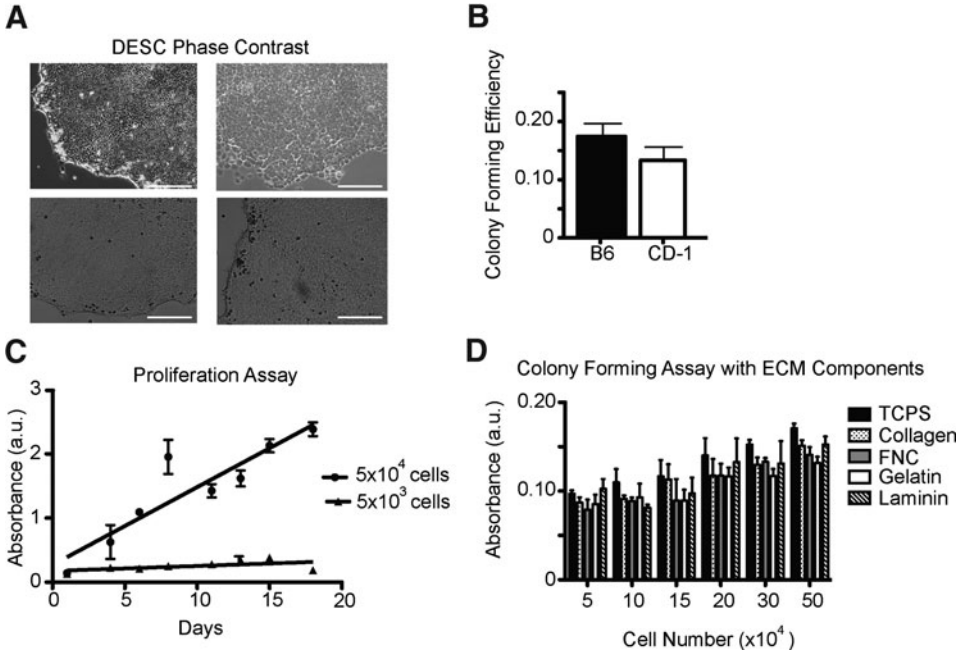

FIG. 2. Characterization of growth rates of DESCs in culture. **(A)** Phase-contrast microscopy of four representative colonies formed *in vitro*. Scale bar = 100 μm. **(B)** Colony-forming capability was compared between two different mouse strains. Efficiency was determined by the number of colonies formed versus the number of cells initially plated. No statistical differences were apparent between the two strains. **(C)** Cell proliferation assay over a period of 20 days with initial cell plating at two different concentrations. Cells plated at 5×10^3/well remained quiescent, with a doubling time of 38 days, while cells plated at 5×10^4/well proliferated, with a doubling time of 2.64 days. **(D)** Colony-forming capability was compared in different cell concentrations on top of various ECM substrates. DESC, dental epithelial stem cell; ECM, extracellular matrix.

In order to identify proteins enriched in DESCs, we examined expression patterns of cell-cell and cell-matrix junctional proteins within cells of the cervical loop. The cell-cell junction protein, E-cadherin, was detected in many regions of the cervical loop, although staining markedly decreased in the T-A region (Fig. 1B, asterisk), which was consistent with previous reports.[21] Beta-catenin, a cell-cell junction linker protein, revealed consistent staining throughout the entire cervical loop region. Integrin alpha-6 protein was located primarily in the outer enamel epithelium and a part of the stellate reticulum (Fig. 1B, arrowhead). Integrin beta-1 protein was located throughout the cervical loop, while integrin beta-4 protein was seen only along the peripheral edges of the cervical loop and in the preameloblast region.

We compared the general morphology and protein expression of the DESCs with two previously reported dental epithelium cell lines. The HAT-7 cell line derived from the cervical loop of 6-day-old rat mandibular incisors was immortalized by serial passaging.[22] The LS8 cell line was derived from mouse molar enamel organ epithelium. This line was immortalized with large T antigen and represents more differentiated cells.[23] Phase-contrast microscopy shows distinct differences in cell morphology among these cell types (Fig. 3A). DESCs formed tightly packed colonies. In contrast, HAT-7 cells displayed a typical epithelial "cobblestone"

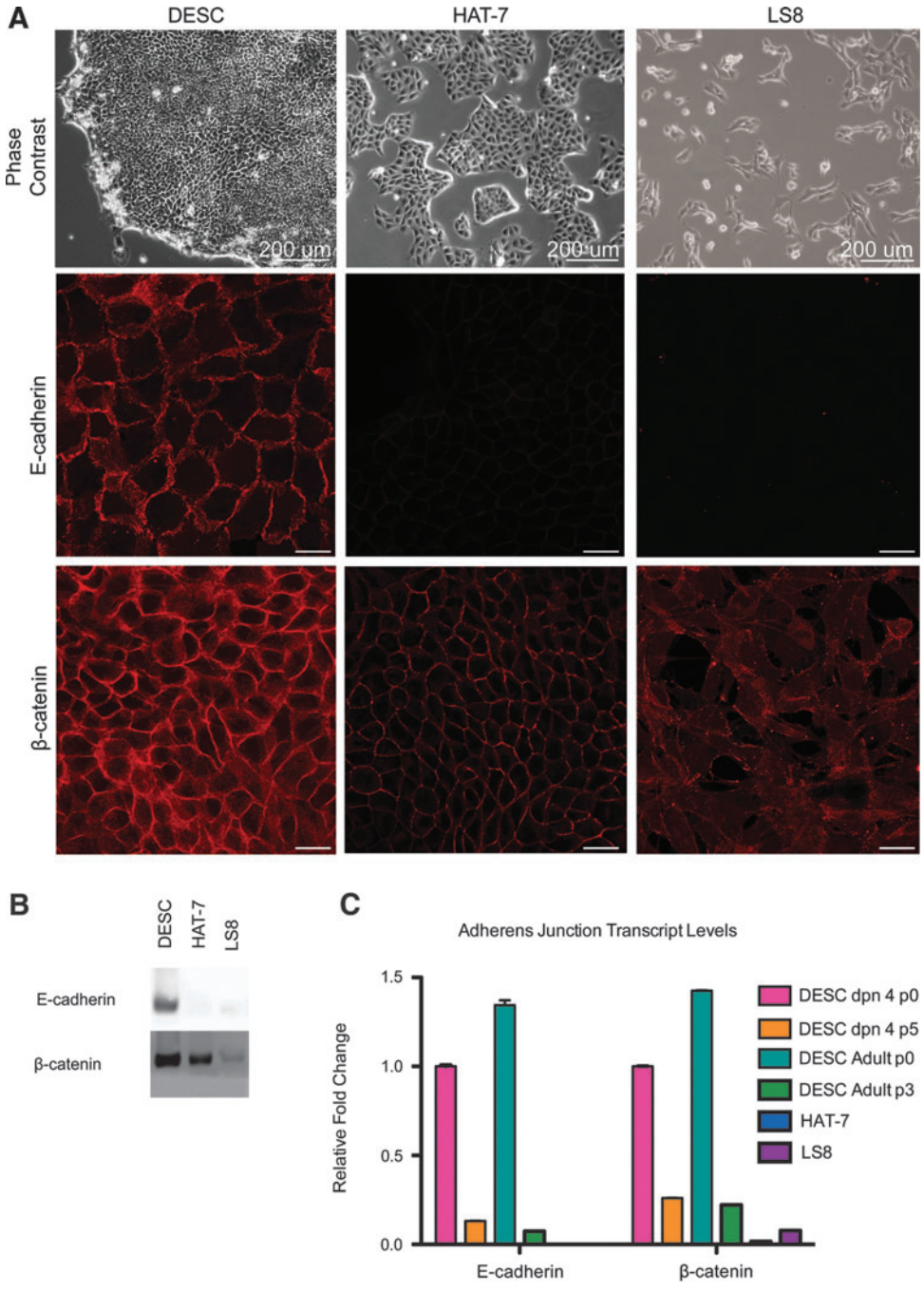

FIG. 3. Characterization of intercellular junction proteins *in vitro.* **(A)** Top row: Phase-contrast microscopy of DESCs, HAT-7 cells, and LS8 cells. Scale bar = 200 μm. Middle row: Immunofluorescence staining of the adherens junction protein E-cadherin. Scale bar = 25 μm. Bottom row: Immunoflorescence staining of beta-catenin. Scale bar = 25 μm. **(B)** Western blots of E-cadherin and beta-catenin protein levels in DESCs, HAT-7 cells, and LS8 cells. **(C)** qPCR for E-cadherin and beta-catenin transcript levels in juvenile and adult mice and at different passages for DESCs, as well as in comparison to HAT-7 and LS8 cells. Expression levels were extremely low for HAT-7 cells (no expression for E-cadherin, beta-catenin = 0.0163, error bars $\pm 0.22 \times 10^{-4}$) as well as LS8 cells (no expression of E-cadherin, beta-catenin = 0.078, error bars $\pm 2.3 \times 10^{-4}$). Adult, at least 21 days old; dpn, day postnatal; p0, initial plating of cells; p3, third passage; p5, fifth passage. All the expression levels were relative to DESC dpn 4 p0. qPCR, quantitative polymerase chain reaction.

morphology, whereas LS8 cells had an elongated cell body, presumably due to their more differentiated status.

Next, all three cell lines were stained for the epithelial cadherin, E-cadherin, and one of its adherens junction binding partners, beta-catenin. Strong staining for E-cadherin at the cell membrane was visible only in the DESCs, whereas such staining was absent in both HAT-7 and LS8 cells. Beta-catenin staining, however, was present in all the cell types tested. Both DESCs and HAT-7 cells showed cell membrane staining of beta-catenin, although the intensity was much greater in DESCs. LS8 cells were also positive for beta-catenin, although it was present in both the cytoplasm and at the cell membrane. In order to confirm the immunofluorescent staining, Western blotting was performed to determine protein levels (Fig. 3B). This assay confirmed that DESCs expressed E-cadherin, whereas no E-cadherin protein was detected in either HAT-7 or LS8 cells. Beta-catenin protein was expressed at highest levels in the DESCs, with progressively lower levels in HAT-7 and LS8 cells, confirming the results observed in immunofluoresence studies.

Since the behavior of stem cells may change as the animal matures, we set out to compare stem cells from juvenile mice with those from adult mice. Expression of E-cadherin and beta-catenin mRNA was measured from DESCs collected from 4-day-old juvenile mice (day postnatal 4 [dpn 4]) as well as adult mice (greater than 21 days old). In addition, we passaged cells several times and compared later passages (designated p3, p5, etc.) with the original passage (p0). All samples were normalized to DESC dpn 4 samples. E-cadherin and beta-catenin transcript levels were highest in the adult DESC p0 population, with slightly lower levels in juvenile p0 transcripts. However, this transcript level decreased after serial passaging, indicating that sustained culture of the stem cells led to significant alterations in the expression of cell adhesion molecules. Interestingly, in all cases, DESCs had higher levels of both E-cadherin and beta-catenin transcripts than HAT-7 and LS8 cells.

The expression of integrins has been successfully used in other systems to identify stem cells. Integrins alpha-6, beta-1, and beta-4 mark embryonic stem cells,[24] lung stem cells[25] and stem cells in the hair bulge.[26] Immunofluoresence staining was positive for alpha-6 integrin in DESCs (Fig. 4A), with little to no staining in the HAT-7 and LS8 cells. Integrin beta-1 staining was strong in both the DESCs and the differentiated LS8 cells, but was absent from the HAT-7 cells. Finally, integrin beta-4 staining was present in DESCs, barely visible in LS8 cells, and largely absent from HAT-7 cells. qPCR results showed the presence of alpha-6 and beta-1 transcripts in HAT-7 cells, although we did not observe evidence for the expression of these proteins by immunofluorescence data (Fig. 4C). This could be due to a lack of translation in these cells, improper export, or problems with antibody recognition. As with the other proteins we examined, alpha-6 transcript levels decreased with serial passage of the DESCs, whether at the juvenile (4 day) or adult (21 day) stage of collection. A similar pattern was true for integrin beta-1. We proceeded to measure protein levels of each integrin by Western blot and found results similar to the immunofluorescence data (Fig. 4B). Integrin alpha 6 and integrin beta-4 proteins were detected solely in DESCs, whereas integrin beta-1 was detected in the DESC and LS8 cells.

Cells were cultured in Matrigel on top of low adherence plates to enable these cells to self arrange in 3D to generate "amelospheres" (Fig. 5A). Several other groups have successfully used this technique with progenitor cells; for example, it is possible to form "mammospheres" from mammary gland stem cells[13,15] and "neurospheres" from neural stem cells.[16,27] Amelospheres were generated after 7–10 days in culture. Plating at different densities from 2×10^3 to 2×10^4 revealed no statistical differences in sphere-forming ability (Fig. 5B). The expression of adherens junction proteins and integrins in cells forming the amelospheres was determined by immunofluorescence staining. Similar to our 2D studies and the *in vivo* findings, amelospheres expressed E-cadherin and beta-catenin as well as integrin alpha-6 (Fig. 5C). Self-renewal was established by dissociation and replating of the cells contributing to the amelospheres into secondary spheres, which was repeated a minimum of twice. Repeated formation of amelospheres showed the ability of DESCs to self-renew in 3D as well as 2D when plated at clonal densities.

Discussion

The rodent incisor houses at least three known stem cell compartments: the lingual and labial cervical loops in the epithelium, as well as a third niche consisting of the mesenchyme enclosed by the cervical loops. Several *in vivo* studies of the rodent incisor, and particularly of the labial cervical loop, have advanced our understanding of the molecular mechanisms regulating continuous incisor growth. Studies implanting cocultures of epithelial and mesenchymal cells from various sources[2,4,8,28–31] have demonstrated that these can give rise to tooth-like, enamel producing-structures, although the exact cell types involved and the molecular mechanisms driving the morphogenesis remain unclear. We endeavored to develop a system that investigates these cells in culture to enable a better understanding of the molecular mechanisms which are responsible for stem cell differentiation and maintenance. Understanding the molecules responsible for stem cell maintenance is an important step toward tissue engineering applications.

We cultured stem cells from the mouse mandible labial cervical loop and found that E-cadherin, beta-catenin, integrin alpha-6, and integrin beta-4 were expressed in the labial cervical loop, and expression of these proteins was maintained in both the 2D and 3D culture systems. E-cadherin was recently found to be an important factor for the maintenance of stem cells in the cervical loop.[21] *In vivo*, E-cadherin is present in the stem cell region, is absent along the area of T-A cells, and reappears in the preameloblast region. Interestingly, conditional knockdown of E-cadherin led to a decrease of label-retaining stem cells and also to a decreased migration of ameloblasts.[21] The expression of these cell adhesion proteins was present throughout the colonies, in contrast to the localized expression in the cervical loop, presumably because the cells have ready access to growth factors from the medium as opposed to the localized expression of such factors seen *in vivo*.

We found that beta-catenin, which binds E-cadherin, was present throughout the cervical loop. However, in the T-A region, where E-cadherin expression is absent, P-cadherin is expressed,[21] explaining the existence of junctional beta-

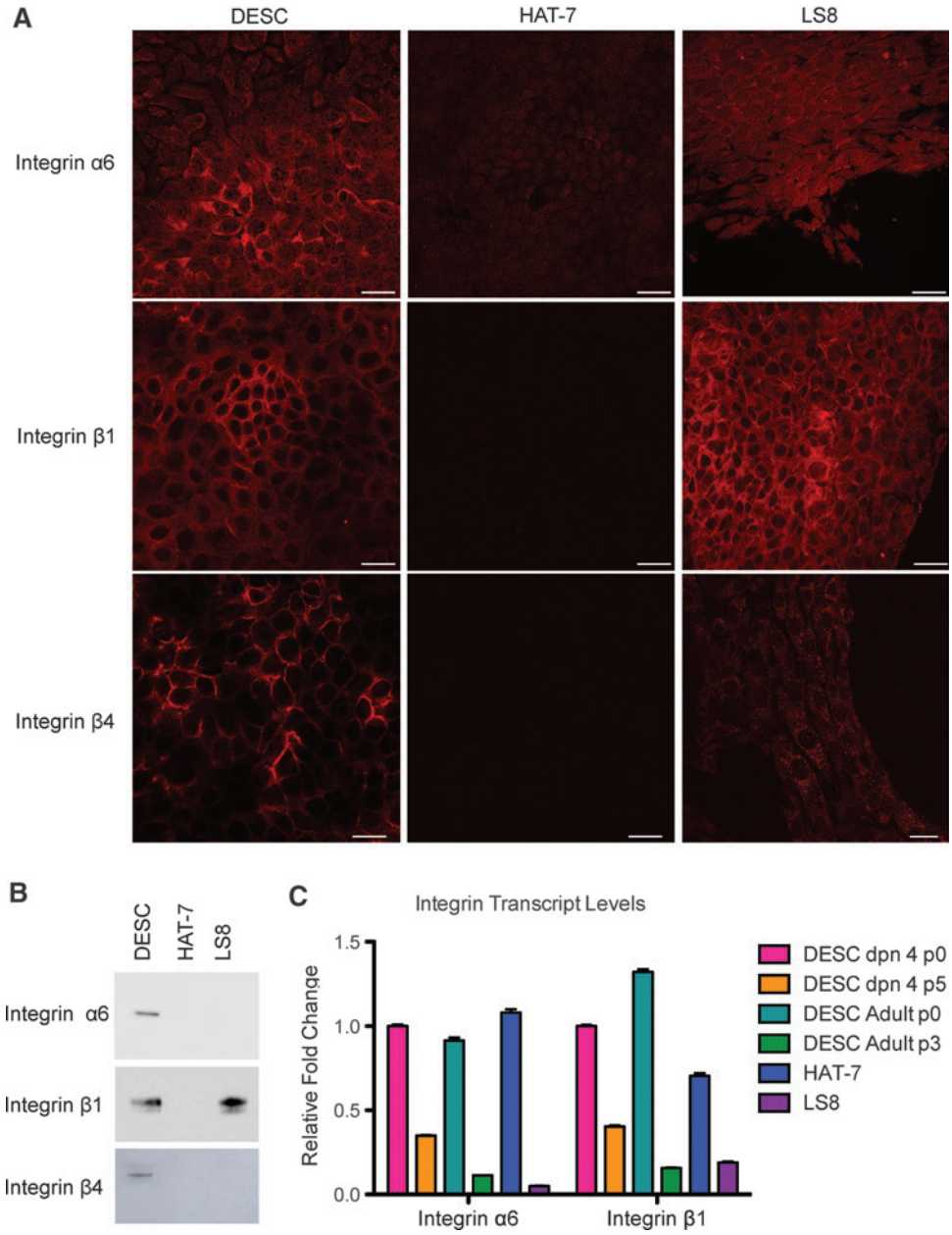

FIG. 4. Characterization of cell-matrix interaction proteins *in vitro.* **(A)** Immunfluorescence staining of integrins in DESC, HAT-7, and LS8 cell lines. Top row: integrin alpha-6; middle row: integrin beta-1; bottom row: integrin beta-4. Scale bar = 25 μm. **(B)** Western blots for protein levels of integrins alpha-6, beta-1, and beta-4 in DESCs and HAT-7 and LS8 cells. **(C)** qPCR for integrins alpha-6 and beta-1 transcript levels in both juvenile and adult mice and at different passages for DESCs as well as in comparison to HAT-7 and LS8 cells. All the expression levels were relative to DESC dpn 4 p0. Color images available online at www.liebertpub.com/tec

catenin with decreased expression of E-cadherin. Beta-catenin is also present in the differentiated cell line LS8, and, thus, is probably not a good candidate as a specific marker for the stem cell population.

Integrin alpha-6 is a surface protein that is expressed in stem cells of the hair bulge,[26] skin,[32] and lung,[25] and in embryonic stem cells.[24] In these systems, integrin alpha-6 positive cells coexpress integrin beta-4[25] or integrin beta-1.[32] We found integrin alpha-6 expression restricted to a localized area in the cervical loop, which coincides with the area where slow-cycling DESCs were previously identified.[33] Both beta-1 and beta-4 integrins were expressed in the cervical loop, and further investigation will be necessary to determine what role these integrins play in stem cell function (Fig. 3C). Significantly, all of these integrin proteins were maintained in both our 2D and 3D culture system and could potentially be useful for the isolation of adult stem cells from the cervical loop. Reliable markers to test whether stem cell self-renewal is maintained in culture are necessary when expanding large amounts of cells for clinical applications, and this step represents a major hurdle in the tissue engineering field.

Integrins bind the cell to extracellular matrix, and, thus, we expected to find preferential colony formation on top of ECM substrates, especially laminin, to which both alpha-6/beta-1 and alpha-6/beta-4 dimers bind. However, we were surprised that we did not identify differences in the colony-forming ability when DESCs were plated on laminin and other ECM substrates, or even on uncoated tissue culture plastic. This could be due to the variability of ECM concentrations deposited or the readout methods employed, which measured absorbance. Methods such as microcontact

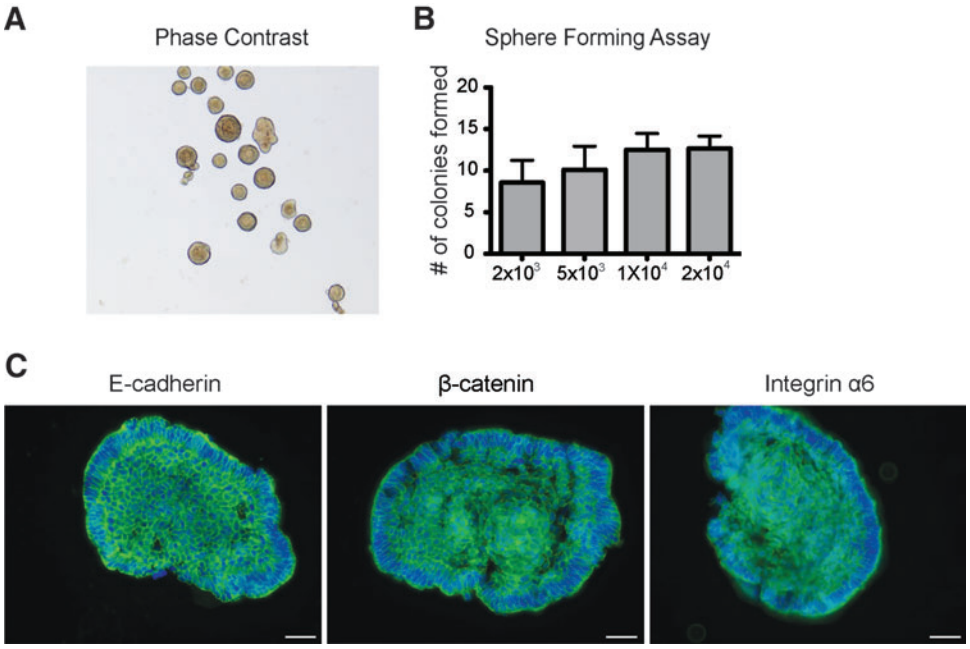

FIG. 5. Primary DESCs can form 3D spheres and self-renew *in vitro.* **(A)** Phase-contrast microscopy image of 3D amelospheres. Spheres formed after 14 days of incubation in Matrigel on top of low adherence plates. **(B)** Sphere-forming assay with different starting concentrations of cells' input. The number of spheres formed was counted after 14 days of incubation on top of low adherence plates. No statistically significant differences were seen with the experimental concentrations tested. **(C)** Immunofluorescence staining of E-cadherin, beta-catenin, and integrin alpha-6 in the 3D amelosphere. Sections were stained with DAPI (blue) to mark nuclei and for E-cadherin, beta-catenin, and Integrin alpha-6. All three proteins were expressed in amelospheres. Scale bar = 25 μm. 3D, three-dimensional. Color images available online at www.liebertpub.com/tec

printing that can deposit defined quantities of ECM, and cell proliferation assays that give more quantitative readouts, will be needed to identify conditions in which the ECM can actually enhance DESC maintenance.

We observed a lower amount of transcription of E-cadherin, beta-catenin, and integrins after several passages of the DESCs. This could be due to fluctuation of cell-cell contacts or altered signaling with an extended culture. However, in all cases, the later passages still maintained higher transcriptional levels of E-cadherin, beta-catenin, and integrin alpha-6 than HAT-7 and LS8 cells. DESCs cultured from our system consistently had higher protein levels of E-cadherin and of integrins alpha-6 and beta-4, compared with HAT-7 and LS8 cells. These proteins were also expressed when the cells were placed in 3D, an important point considering that in many other systems, when culture conditions are changed from 2D to 3D, marker expression is lost.[34,35] The use of DESCs from primary culture yields cells that more closely resemble those found *in vivo* compared with the immortalized HAT-7 cells. It is certainly the case that the cells we have isolated contain subpopulations of stem cells, and it is also likely that there is some low-level contamination with other cell types. Therefore, future work will be required to develop techniques in which purified or sorted cells are used. Nevertheless, we expect that for many applications, the dissection-based technique that we report here will prove useful, as the limited quantities of cells which are obtainable after sorting may not be sufficient in many cases.

An interesting difference was seen in the proliferation rates of DESCs in 2D and 3D when plated at varying concentrations. In 2D, there was a dramatic decrease in proliferation when the concentration of cells was lowered from 5×10^4 to 5×10^3 (2.64 days vs. 38 days doubling time). In 3D, however, a change from 2×10^4 to 2×10^3 did not cause any statistically significant change in the sphere-forming capability. We suggest that the improved conditions provided by the 3D environment account for this difference.

In conclusion, we have developed a robust system for culturing DESCs from the mouse mandibular incisor. DESC colonies formed using samples harvested from different strains of mice, on top of a variety of ECM substrates, and expressing several proteins found in the stem cell niche *in vivo*. Understanding the maintenance of adult DESCs may provide knowledge that will enable rationally designed tissue-engineered constructs.

Acknowledgments

The authors thank X.-P. Wang, K. Seidel, and A. Jheon for technical assistance; D.A. Bernards for critiquing the article; and members of the Klein and Desai laboratories for helpful discussions. M.G.C. was funded by Grant Number K12GM081266 from the National Institute of General Medical Sciences (NIGMS)/National Institutes of Health. The contents of this article are solely the responsibility of the authors and do not necessarily represent the official views of the NIGMS. M.L.S. was supported by DE06988 from the National Institute for Dental and Craniofacial Research of the National Institutes of Health. This work was funded by a New Faculty Award II (RN2-00933) from the California

Institute for Regenerative Medicine to O.D.K. and by the National Institutes of Health through the NIH Director's New Innovator Award Program, 1-DP2-OD007191 and R01-DE021420, both to O.D.K.

Disclosure Statement

No competing financial interests exist.

References

1. Atala, A. Engineering organs. Curr Opin Biotechnol **20,** 575, 2009.
2. Duailibi, M.T., Duailibi, S.E., Young, C.S., Bartlett, J.D., Vacanti, J.P., and Yelick, P.C. Bioengineered teeth from cultured rat tooth bud cells. J Dent Res **83,** 523, 2004.
3. Sonoyama, W., Liu, Y., Fang, D., Yamaza, T., Seo, B.M., Zhang, C., *et al.* Mesenchymal stem cell-mediated functional tooth regeneration in swine. PLoS One **1,** e79, 2006.
4. Ikeda, E., Morita, R., Nakao, K., Ishida, K., Nakamura, T., Takano-Yamamoto, T., *et al.* Fully functional bioengineered tooth replacement as an organ replacement therapy. Proc Natl Acad Sci U S A **106,** 13475, 2009.
5. Guo, W., Chen, L., Gong, K., Ding, B., Duan, Y., and Jin, Y. Heterogeneous dental follicle cells and the regeneration of complex periodontal tissues. Tissue Eng Part A **18,** 459, 2012.
6. Yamaza, T., Ren, G., Akiyama, K., Chen, C., Shi, Y., and Shi, S. Mouse mandible contains distinctive mesenchymal stem cells. J Dent Res **90,** 317, 2011.
7. Takahashi, C., Yoshida, H., Komine, A., Nakao, K., Tsuji, T., and Tomooka, Y. Newly established cell lines from mouse oral epithelium regenerate teeth when combined with dental mesenchyme. In Vitro Cell Dev Biol Anim **46,** 457, 2010.
8. Xiao, L., and Tsutsui, T. Three-dimensional epithelial and mesenchymal cell co-cultures form early tooth epithelium invagination-like structures: expression patterns of relevant molecules. J Cell Biochem **113,** 1875, 2012.
9. Smith, C.E., and Warshawsky, H. Quantitative analysis of cell turnover in the enamel organ of the rat incisor. Evidence for ameloblast death immediately after enamel matrix secretion. Anat Rec **187,** 63, 1977.
10. Tummers, M., and Thesleff, I. Root or crown: a developmental choice orchestrated by the differential regulation of the epithelial stem cell niche in the tooth of two rodent species. Development **130,** 1049, 2003.
11. Harada, H., Kettunen, P., Jung, H.S., Mustonen, T., Wang, Y.A., and Thesleff, I. Localization of putative stem cells in dental epithelium and their association with Notch and FGF signaling. J Cell Biol **147,** 105, 1999.
12. Smith, C.E., and Warshawsky, H. Cellular renewal in the enamel organ and the odontoblast layer of the rat incisor as followed by radioautography using 3H-thymidine. Anat Rec **183,** 523, 1975.
13. Woodward, W.A., Chen, M.S., Behbod, F., and Rosen, J.M. On mammary stem cells. J Cell Sci **118,** 3585, 2005.
14. Lin, R.Z., and Chang, H.Y. Recent advances in three-dimensional multicellular spheroid culture for biomedical research. Biotechnol J **3,** 1172, 2008.
15. Dontu, G., Abdallah, W.M., Foley, J.M., Jackson, K.W., Clarke, M.F., Kawamura, M.J., *et al. In vitro* propagation and transcriptional profiling of human mammary stem/progenitor cells. Genes Dev **17,** 1253, 2003.
16. Ahmed, S. The culture of neural stem cells. J Cell Biochem **106,** 1, 2009.
17. Morotomi, T., Kawano, S., Toyono, T., Kitamura, C., Terashita, M., Uchida, T., *et al. In vitro* differentiation of dental epithelial progenitor cells through epithelial-mesenchymal interactions. Arch Oral Biol **50,** 695, 2005.
18. Franken, N.A., Rodermond, H.M., Stap, J., Haveman, J., and van Bree, C. Clonogenic assay of cells *in vitro*. Nat Protoc **1,** 2315, 2006.
19. Tumbar, T., Guasch, G., Greco, V., Blanpain, C., Lowry, W.E., Rendl, M., *et al.* Defining the epithelial stem cell niche in skin. Science **303,** 359, 2004.
20. Jensen, K.B., Driskell, R.R., and Watt, F.M. Assaying proliferation and differentiation capacity of stem cells using disaggregated adult mouse epidermis. Nat Protoc **5,** 898, 2010.
21. Li, C-Y., Cha, W., Luder, H.U., Charles, R.P., McMahon, M., and Klein, O.D. E-cadherin regulates the behavior and fate of epithelial stem cells and their progeny in the mouse incisor. Dev Biol **366,** 357, 2012.
22. Kawano, S., Morotomi, T., Toyono, T., Nakamura, N., Uchida, T., Ohishi, M., *et al.* Establishment of dental epithelial cell line (HAT-7) and the cell differentiation dependent on Notch signaling pathway. Connect Tissue Res **43,** 409, 2002.
23. Chen, L.S., Couwenhoven, R.I., Hsu, D., Luo, W., and Snead, M.L. Maintenance of amelogenin gene expression by transformed epithelial cells of mouse enamel organ. Arch Oral Biol **37,** 771, 1992.
24. Yu, K.R., Yang, S.R., Jung, J.W., Kim, H., Ko, K., Han, D.W., *et al.* CD49f enhances multipotency and maintains stemness through the direct regulation of OCT4 and SOX2. Stem Cells **30,** 876, 2012.
25. Chapman, H.A., Li, X., Alexander, J.P., Brumwell, A., Lorizio, W., Tan, K., *et al.* Integrin alpha6beta4 identifies an adult distal lung epithelial population with regenerative potential in mice. J Clin Invest **121,** 2855, 2011.
26. Blanpain, C., Lowry, W.E., Geoghegan, A., Polak, L., and Fuchs, E. Self-renewal, multipotency, and the existence of two cell populations within an epithelial stem cell niche. Cell **118,** 635, 2004.
27. Conti, L., and Cattaneo, E. Neural stem cell systems: physiological players or *in vitro* entities? Nat Rev Neurosci **11,** 176, 2010.
28. Young, C.S., Abukawa, H., Asrican, R., Ravens, M., Troulis, M.J., Kaban, L.B., *et al.* Tissue-engineered hybrid tooth and bone. Tissue Eng **11,** 1599, 2005.
29. Abukawa, H., Zhang, W., Young, C.S., Asrican, R., Vacanti, J.P., Kaban, L.B., *et al.* Reconstructing mandibular defects using autologous tissue-engineered tooth and bone constructs. J Oral Maxillofac Surg **67,** 335, 2009.
30. Oshima, M., Mizuno, M., Imamura, A., Ogawa, M., Yasukawa, M., Yamazaki, H., *et al.* Functional tooth regeneration using a bioengineered tooth unit as a mature organ replacement regenerative therapy. PLoS One **6,** e21531, 2011.
31. Guo, W., Gong, K., Shi, H., Zhu, G., He, Y., Ding, B., *et al.* Dental follicle cells and treated dentin matrix scaffold for tissue engineering the tooth root. Biomaterials **33,** 1291, 2012.
32. Schober, M., and Fuchs, E. Tumor-initiating stem cells of squamous cell carcinomas and their control by TGF-beta and integrin/focal adhesion kinase (FAK) signaling. Proc Natl Acad Sci U S A **108,** 10544, 2011.

33. Seidel, K., Ahn, C.P., Lyons, D., Nee, A., Ting, K., Brownell, I., *et al.* Hedgehog signaling regulates the generation of ameloblast progenitors in the continuously growing mouse incisor. Development **137,** 3753, 2010.
34. Lu, H., Searle, K., Liu, Y., and Parker, T. The effect of dimensionality on growth and differentiation of neural progenitors from different regions of fetal rat brain *in vitro*: 3-dimensional spheroid versus 2-dimensional monolayer culture. Cells Tissues Organs **196,** 48, 2012.
35. Liu, H., and Roy, K. Biomimetic three-dimensional cultures significantly increase hematopoietic differentiation efficacy of embryonic stem cells. Tissue Eng **11,** 319, 2005.

Address correspondence to:
Ophir D. Klein, M.D., Ph.D.
Departments of Orofacial Sciences and Pediatrics
Program in Craniofacial and Mesenchymal Biology
University of California San Francisco
San Francisco, CA 94143

E-mail: ophir.klein@ucsf.edu

Received: April 11, 2012
Accepted: June 5, 2012
Online Publication Date: August 15, 2012